Research Square

Preprints are preliminary reports that have not undergone peer review.
They should not be considered conclusive, used to inform clinical practice,
or referenced by the media as validated information.

Sequential combination treatment with TKIs and anti-PD-1 therapy in TKI-responsive patients with metastatic MSS/pMMR colorectal cancer: an open-label, single-arm phase 2 trial

Jingdong Zhang

jdzhang@cancerhosp-ln-cmu.com

Cancer Hospital of Dalian University of Technology, Liaoning Cancer Hospital & Institute
https://orcid.org/0000-0002-0711-2764

Qian Dong

Cancer Hospital of Dalian University of Technology, Liaoning Cancer Hospital & Institute
https://orcid.org/0000-0001-9810-1368

Yanwen Diao

Cancer Hospital of Dalian University of Technology, Liaoning Cancer Hospital & Institute

Xin Sun

Cancer Hospital of Dalian University of Technology, Liaoning Cancer Hospital & Institute

Haobo Yin

Cancer Hospital of Dalian University of Technology, Liaoning Cancer Hospital & Institute

Xiujie Cui

Chaoyang Central Hospital

Jin Zhou

Cancer Hospital of Dalian University of Technology, Liaoning Cancer Hospital & Institute

Lingshan Wang

Cancer Hospital of Dalian University of Technology, Liaoning Cancer Hospital & Institute

Jian Zhang

Liaoyang Central Hospital of China Medical University

Li Man

Anshan Cancer Hospital

Yuyang Zhang

General Hospital of Fushun Mining Bureau of Liaoning Health Industry Group

Yuanhe Wang

Cancer Hospital of Dalian University of Technology, Liaoning Cancer Hospital & Institute
https://orcid.org/0000-0002-0012-1756

Tao Wu

the Second Hospital of Dalian Medical University

Tiejun Chen

Benxi Central Hospital

Yuyang Dong

Anshan Cancer Hospital

Junwei Zhang

Panjin Central Hospital

Yanyuan Huang

Liaoyang county Central Hospital

Siliang Wang

Shengjing Hospital of China Medical University

Hongming Xu

School of Biomedical Engineering, Faculty of Medicine, Dalian University of Technology

https://orcid.org/0000-0002-1305-0010

Xiaorui Ma

Cancer Hospital of Dalian University of Technology

Article

Keywords: tyrosine kinase inhibitors (TKIs) , anti-programmed cell death protein 1 (PD-1), metastatic colorectal cancer (mCRC), microsatellite stable/proficient mismatch repair (MSS/pMMR), TRAP trial

Posted Date: October 27th, 2026

DOI: https://doi.org/10.21203/rs.3.rs-10842327/v1

License: This work is licensed under a Creative Commons Attribution 4.0 International License.
Read Full License

Additional Declarations: There is **NO** Competing Interest.

Abstract

Patients with microsatellite-stable/proficient mismatch repair (MSS/pMMR) metastatic colorectal cancer derive limited benefit from immune checkpoint inhibitors. In this multicentre phase 2 trial, patients received tyrosine kinase inhibitors (TKIs) fruquintinib or regorafenib during screening; radiological responders received TKI plus anti-programmed cell death protein 1 (PD-1) therapy. Of 60 enrolled patients, 25 received the sequential combination; the 9-month progression-free survival (PFS) rate, the prespecified primary endpoint, was 57.7%; median PFS and overall survival were 12.5 and 22.4 months (median follow-up, 24.4 months). Objective response and disease control rates were 20.0% and 100.0%; grade ≥3 treatment-related adverse events affected 48.0% of patients, with no treatment-related deaths. Baseline radiomics predicted benefit (area under the curve, 0.75), and dynamic changes in radiomics, circulating tumour DNA and T-cell receptor repertoire followed TKI priming. Sequential TKI priming followed by TKI plus anti-PD-1 therapy showed encouraging activity and manageable toxicity, supporting response-adapted sequential immunotherapy in this population.

Clinical trial registration: NCT04483219 (registered 23 July 2020)

Introduction

Immunotherapy has shown limited efficacy in microsatellite stable/proficient mismatch repair (MSS/pMMR) metastatic colorectal cancer (mCRC), which represents the majority of advanced colorectal cancers[1–3]. Although multiple combination strategies have been explored to overcome immune resistance, including anti-angiogenic agents and epigenetic therapies, durable clinical benefit has remained inconsistent in unselected MSS/pMMR populations[4–8]. Reliable biomarkers for identifying patients most likely to benefit from immunotherapy-based combinations are also lacking[9,10].

Among currently investigated approaches, combinations of tyrosine kinase inhibitors (TKIs) and immune checkpoint inhibitors (ICIs) have demonstrated preliminary activity in selected patients with MSS/pMMR mCRC. Regorafenib- and fruquintinib-based combinations have shown encouraging signals in early-phase studies; however, clinical outcomes across trials have varied substantially, suggesting that only a subset of patients derive meaningful benefit[11–13]. In addition to concurrent combination strategies, sequential therapeutic approaches have also gained increasing interest. Notably, the MAYA trial demonstrated the feasibility of a response-adapted sequential immunotherapy strategy in colorectal cancer, supporting further investigation of treatment sequencing approaches[14].

Fruquintinib and regorafenib are standard later-line treatment options for previously treated MSS/pMMR mCRC. Beyond their anti-angiogenic activity, preclinical and clinical observations suggest that TKIs exposure may modulate tumour and immune microenvironmental features associated with sensitivity to immune checkpoint blockade[15]. Retrospective and early-phase studies have suggested that selected patients achieving disease control during TKIs treatment may subsequently derive benefit from

immunotherapy-based combinations[16–18]. These observations raise the possibility that response to initial TKIs treatment may identify a subgroup potentially sensitive to subsequent PD-1 blockade.

Based on this rationale, we conducted the prospective multicentre phase 2 TRAP trial to evaluate the efficacy and safety of sequential TKIs followed by TKIs plus anti-programmed cell death protein 1 (PD-1) therapy in patients with MSS/pMMR mCRC who achieved radiological response to initial TKIs treatment.

Results

Patients and treatment

The patient disposition is shown in Figure 1. Between 10 March 2021 and 24 June 2024, 60 eligible patients were enrolled, of whom 58 initiated TKIs treatment. Following the initial TKIs treatment phase, 24 patients met the predefined radiological criteria for assignment to arm A. Among the remaining patients, 12 were assigned to arm B and 22 to arm C. After the second treatment cycle, one patient from arm B was reassigned to arm A based on subsequent imaging evaluation. Consequently, 25 patients were included in the arm A intention-to-treat and safety populations.

At the data cutoff date of 23 December 2025, 21 patients (84.0%) in arm A had discontinued treatment because of disease progression, three (12.0%) because of treatment-related adverse events, and one (4.0%) because of an acute myocardial infarction considered unrelated to study treatment.

Baseline characteristics are summarised in Table 1. In arm A, the median age was 57 years (range, 34–74 years), and 15 patients (60.0%) were male. Most patients had an ECOG performance status of 1 (96.0%), left-sided primary tumours (88.0%), and lung metastases (80.0%). RAS mutations were identified in nine patients (36.0%), and BRAFV600E mutations in two (8.0%). Most patients had received fewer than three prior lines of systemic therapy.

Clinical activity

After a median follow-up of 24.39 months, the median progression-free survival (PFS) in arm A was 12.49 months (95% CI, 7.31–18.56), and the median overall survival (OS) was 22.43 months (95% CI, 16.92–28.95) . In comparison, median PFS and OS were 1.87 months (95% CI, 1.84–2.72) and 13.41 months (95% CI, 5.51–16.30) in arm B, and 0.97 months (95% CI, 0.92–1.02) and 10.03 months (95% CI, 5.28 –12.89) in arm C, respectively. In arm A, the 9-month PFS rate was 57.69% (95% CI, 34.34–75.35), indicating that the prespecified primary endpoint was met. Twenty-one PFS events (84.0%) were observed at the data cutoff date. (Figure 2A-B)

Exploratory analyses suggested associations between survival outcomes and metastatic burden. Patients with single-organ metastasis demonstrated longer median PFS than those with multi-organ metastases (18.56 months [95% CI, 4.85–NE] vs 8.62 months [95% CI, 6.82–13.11]). Patients without

liver metastases also demonstrated longer median PFS than those with liver metastases. No other clinicopathological variables were significantly associated with survival outcomes (Figure S1).

Among patients in arm A, five (20.0%) achieved a partial response and 20 (80.0%) achieved stable disease according to iRECIST v1.1, resulting in an objective response rate of 20.0% (95% CI, 6.8–40.7) and a disease control rate of 100.0% (95% CI, 86.3–100.0). The median duration of response was 8.08 months (95% CI, 2.10–NE). Tumour shrinkage was observed in 16 patients (64.0%). (Figure 2C-E) Selected radiographic changes during treatment, including cavitation of pulmonary metastases and reduced liver lesion density, were observed in a subset of patients (Figure S2).

Post-study treatment was administered to 16 patients, including targeted therapy in 13 (81.25%), chemotherapy in 14 (87.5%), immunotherapy in two (12.5%) and radiotherapy in two (12.5%) patients.

Safety

Treatment-emergent adverse events (TEAEs) occurring in arm A are summarised in Table 2. The most common TEAEs were palmar-plantar erythrodysesthesia (32.0%), hypertension (28.0%), proteinuria (24.0%), hypothyroidism (24.0%), hoarseness (16.0%), pneumonitis (12.0%), and fatigue (12.0%). Grade ≥3 treatment-related adverse events occurred in 12 patients (48.0%), most commonly hypertension (16.0%). Three patients (12.0%) discontinued treatment because of adverse events, including myocarditis and myositis. No treatment-related deaths were observed.

During the TKI screening phase, TRAEs were systematically recorded to assess both safety and individual tolerability. The most common toxicity-induced symptoms were hypertension, palmar-plantar erythrodysesthesia, proteinuria, fatigue, arthralgia and hoarseness. Grade ≥3 adverse events, including hypertension (n = 3) and palmar-plantar erythrodysesthesia (n = 1), occurred in a subset of patients. Grade 2 toxic effects included proteinuria, palmar-plantar erythrodysesthesia, hypertension and fatigue. Grade 1 toxic effects were generally mild and manageable.Based on individual tolerability, six patients underwent TKI dose reductions during the screening phase, allowing optimization of treatment exposure before combination therapy.

Immune-related adverse events (irAEs) were primarily hypothyroidism (24% any grade, 4% grade ≥3), myocarditis (8%, 4%), hyperthyroidism (8%, 0%) and myositis (8%, 4%). Less frequent irAEs included adrenal insufficiency (4%, 4%), elevated creatinine levels (4%, 4%), hypophysitis (4%, 0%), pneumonitis (4%, 0%), hepatic injury (4%, 0%), anorexia (4%, 0%), weight loss (4%, 0%) and palmar-plantar erythrodysesthesia (4%, 0%). There were no fatal irAEs.

Radiomics

Baseline computed tomography imaging data were available for 50 of 55 evaluable patients, including longitudinal paired imaging data from 24 patients in arm A. Exploratory radiomics analyses were

performed to investigate imaging features associated with clinical benefit from sequential combination therapy.

Baseline radiomics model for predicting clinical benefit from sequential combination immunotherapy

A radiomics model constructed using baseline imaging data from 50 patients demonstrated moderate discriminatory performance for identifying patients assigned to arm A versus arms B and C, with an area under the curve of 0.75. These findings suggest that baseline imaging phenotypes associated with tumour heterogeneity may be associated with benefit from sequential TKIs plus anti-PD-1 therapy. (Figure 3A-D)

Dynamic radiomic changes following TKIs treatment

We performed paired analysis of radiomics features before and after TKIs treatment in arm A patients. After correction for multiple testing, a subset of radiomic features remained statistically significant (adjusted p of <0.05). (Figure 3E) These predominantly involved grey-level distribution, texture heterogeneity and multiscale texture patterns derived from wavelet and LoG filters. Representative significant features included grey-level non-uniformity, dependence non-uniformity, zone variance and large area high grey-level emphasis. Functionally, these altered features were primarily associated with tumour density distribution and spatial heterogeneity. The changes in grey-level-related features suggest remodelling of intratumoral density, potentially reflecting increased necrosis or a reduction in viable tumour components. The reduction in heterogeneity-related metrics (e.g. non-uniformity and variance) indicates a shift towards more homogeneous intratumoral architecture. In addition, several features derived from wavelet- and LoG-filtered images remained significant after adjustment. This suggests that treatment-related changes extend beyond global intensity shifts to involve microstructural remodelling across multiple spatial scales. Collectively, these dynamic radiomic changes appear to reflect improved perfusion uniformity and redistribution within the tumour microenvironment. This indirectly suggests possible treatment-induced vascular normalisation.

Early multiomics changes following TKIs therapy

Peripheral blood samples were collected from patients in Arm A at baseline, after one cycle of TKI treatment, and at disease progression for exploratory multiomics analyses. Serial blood samples available at all three time points were obtained from 8 patients for dynamic ctDNA profiling and T-cell receptor (TCR) repertoire analysis. (Figure 4)

Early decreases in ctDNA levels were observed following initiation of TKIs treatment, consistent with early reductions in tumour burden. TCR repertoire analyses demonstrated dynamic changes in clonality-related metrics after TKIs exposure, suggesting treatment-associated modulation of systemic immune profiles.

Collectively, these findings suggest that TKIs priming may be associated with alterations in tumour and immune microenvironment-related biological processes.

Finally, a representative participant from the TRAP cohort is presented to illustrate the complete treatment trajectory, encompassing radiological responses during the TKI screening phase and treatment period, as well as dynamic molecular biomarker changes. (Figure S3)

Discussion

In this prospective multicentre phase 2 TRAP trial, a response-adapted sequential strategy consisting of TKI priming followed by TKI plus anti-PD-1 therapy demonstrated potent anti-tumour activity and manageable toxicity in selected patients with MSS/pMMR mCRC. The study met its primary endpoint, achieving a 9-month PFS rate of 57.69%, with a median PFS of 12.49 months and a median OS of 22.43 months. These findings suggest that early radiological benefit from TKI treatment may identify a subgroup of patients with MSS/pMMR mCRC who are more likely to derive clinically meaningful benefit from subsequent immunotherapy-based treatment.

Despite major advances in immunotherapy across multiple tumour types, MSS/pMMR mCRC remains largely refractory to immune checkpoint blockade[19–21]. Numerous combination strategies have therefore been investigated to overcome this resistance, including anti-angiogenic agents, epigenetic therapies, and multikinase inhibitors[22–24]. Combinations of TKIs and PD-1 inhibitors have particularly garnered substantial interest. The REGONIVO study initially reported promising anti-tumour activity of regorafenib plus nivolumab against MSS mCRC; however, subsequent validation studies yielded variable outcomes, suggesting that benefit may be confined to specific patient subsets[12]. Similarly, although the CAPABILITY-01 study demonstrated encouraging activity with chidamide-based regimens, treatment efficacy remained heterogeneous across different cohorts[8]. Collectively, these studies suggest that patient selection represents a critical determinant of treatment efficacy in MSS/pMMR disease.

In this context, the TRAP study differs from previous approaches by incorporating a response-adapted treatment strategy. Rather than administering immunotherapy to an unselected population, patients were first exposed to TKIs and subsequently selected for combination treatment according to predefined radiological criteria. A similar response-adapted principle was explored in the MAYA trial, wherein patients with MGMT-silenced MSS colorectal cancer who demonstrated sensitivity to temozolomide subsequently achieved meaningful benefit from dual immune checkpoint blockade[14]. Although the biological context differs substantially from that of the present study, both trials support the broader concept that response to an initial priming treatment may identify tumours with enhanced susceptibility to subsequent immunotherapy. The favourable survival outcomes observed in our study therefore support further investigation of TKI responsiveness as a clinically relevant indicator of potential immunotherapy benefit.

A notable feature of our study is the use of routine radiological assessment as a dynamic selection strategy. In addition to conventional RECIST responses, imaging characteristics associated with anti-angiogenic activity, including cavitation of pulmonary metastases and reductions in liver lesion density, were incorporated into treatment decision-making[25–27]. These imaging changes may reflect biological

effects of angiogenesis inhibition, including tumour necrosis, altered vascular permeability and tumour microenvironment remodelling[28]. Compared with tissue-based biomarkers, which often require specialised testing and are present in only a small subset of MSS/pMMR tumours, imaging-based assessment is readily available, inexpensive and broadly applicable in routine clinical practice. The imaging-based response criteria used in this study were prospectively defined according to biological characteristics associated with anti-angiogenic treatment response; however, further external validation and assessment of interobserver reproducibility will be required before broader implementation. Nevertheless, our findings suggest that treatment-induced radiological changes may represent a practical biomarker for identifying patients most likely to benefit from subsequent immunotherapy.

The safety profile of sequential TKI plus anti-PD-1 therapy was consistent with the known toxicities of the individual agents, and no new safety signals were observed. Most TRAEs were manageable with standard supportive measures or immunosuppressive therapy when indicated, and no treatment-related deaths occurred. The initial TKI screening phase may also have facilitated individualised dose adjustment before initiation of combination therapy, potentially contributing to the acceptable safety profile observed in this study.

To further explore the biological basis of clinical benefit, we performed exploratory radiomic and multiomics analyses. Baseline radiomic features demonstrated moderate ability to identify patients who subsequently derived benefit from sequential immunotherapy, while longitudinal radiomic analyses revealed significant changes in tumour heterogeneity following TKI exposure. In parallel, early reductions in ctDNA levels and alterations in TCR repertoire metrics were observed after TKI treatment. Although these findings are exploratory and based on limited sample sizes, they collectively suggest that TKI priming may induce biological changes within the tumour and immune microenvironment that may be associated with subsequent responsiveness to PD-1 blockade. These observations should be considered hypothesis-generating and warrant validation in larger prospective cohorts.

Several biological mechanisms may potentially contribute to the observed clinical activity. Preclinical studies have demonstrated that TKIs can promote tumour antigen release through tumour cell death, normalise abnormal tumour vasculature, improve immune-cell trafficking, and enhance anti-tumour immune responses[24,29]. In addition, preclinical evidence suggests that TKIs may reduce immunosuppressive cellular populations within the tumour microenvironment[30,31]. Together, these effects may create a more permissive immune context for subsequent checkpoint inhibition. Although our exploratory biomarker analyses are broadly consistent with this hypothesis, definitive mechanistic conclusions cannot be established from the current study, warranting dedicated translational investigations.

This study has several limitations. First, as a single-arm phase 2 trial, comparisons with historical studies should be interpreted cautiously. Second, the sample size was relatively small, particularly for subgroup analyses and exploratory biomarker investigations. Third, the imaging-based criteria used to define TKI responsiveness were investigator-defined and require prospective validation and

standardisation in independent cohorts. Fourth, biomarker analyses were conducted in only a subset of patients and should therefore be considered exploratory. Finally, all participants were enrolled in China, which may limit the generalisability of the findings to other populations.

In conclusion, the TRAP trial demonstrates that a response-adapted sequential strategy of TKI priming followed by TKI plus anti-PD-1 therapy can achieve durable clinical benefit with manageable toxicity in selected patients with MSS/pMMR mCRC. Beyond the efficacy results, the study highlights the potential value of treatment-induced radiological changes as a practical and clinically accessible biomarker for patient selection. If confirmed in future randomised studies, this strategy may represent a practical approach for enriching immunotherapy-responsive populations in a disease historically characterised by resistance to immune checkpoint blockade and may contribute to the development of more precise treatment paradigms for MSS/pMMR mCRC.

Methods

Patients Eligibility

Eligible patients were aged 18–75 years, had an Eastern Cooperative Oncology Group performance status (ECOG PS) of 0–1, histologically confirmed unresectable or metastatic adenocarcinoma of the colon or rectum, measurable disease according to RECIST version 1.1, and previously treated MSS/pMMR metastatic colorectal cancer. MSS/pMMR status was confirmed by immunohistochemistry, polymerase chain reaction, or next-generation sequencing. All patients had received standard fluoropyrimidine-, oxaliplatin-, and irinotecan-based therapies, with or without prior anti-VEGF or anti-EGFR treatment, as appropriate. Detailed eligibility criteria are provided in the study protocol (doi:10.1136/bmjopen-2021-049992).

Study Design and Procedures

TRAP was an investigator-initiated, prospective, multicentre, open-label, single-arm phase 2 trial (ClinicalTrials.gov identifier: NCT04483219, registered 23 July 2020). The study was conducted at eight centres in China in accordance with the Declaration of Helsinki and Good Clinical Practice guidelines. The protocol was approved by the institutional ethics committee of each participating centre, and all patients provided written informed consent before enrolment.

The study employed a response-adapted sequential treatment strategy. During an initial screening phase, patients received one cycle of fruquintinib or regorafenib. Radiological assessment was performed after completion of the screening cycle.

According to their response to TKIs, patients were divided into three arms: (1) Arm A: an obvious response to TKIs, including reduction in the diameter of target lesions, to complete response (CR), partial response (PR) or shrunken SD, according to the revised Response Evaluation Criteria in Solid Tumors (RECIST) guidelines (version 1.1). In addition, patients without progressive disease (non-PD) who

exhibited specific radiographic changes suggestive of treatment response—such as cavitation of solid metastatic lung lesions or a ≥ 15% decrease in the density of metastatic liver lesions according to Choi criteria were also classified into Arm A. (2) Arm B: general response to TKIs, including enlarged SD and without the radiographic features described for Arm A (based on RECIST version 1.1 guidelines). (3) Arm C: poor response to TKIs, including progressive disease (based on RECIST version 1.1 guidelines). Patients assigned to arm A subsequently received TKIs in combination with an anti-PD-1 antibody. Patients assigned to arm B continued TKI treatment for one additional cycle and underwent repeat assessment. Patients demonstrating subsequent radiological benefit were reassigned to arm A. Patients in arm C discontinued protocol treatment. Treatment continued until disease progression, unacceptable toxicity, withdrawal of consent, or investigator decision. Anti-PD-1 therapy was administered for a maximum duration of two years.

Assessments

Tumour imaging assessments were performed every 4 weeks during the first two treatment cycles and every 6 weeks thereafter. Response to TKIs was assessed according to the RECIST criteria (version 1.1) and significant changes in imaging findings (cavitation in metastatic lung lesions or a decrease in the density of liver metastatic targeted lesions ≥ 15%). In addition, the efficacy of TKIs followed by TKIs in combination with anti-PD-1 antibody is assessed based on the immune-related RECIST (iRECIST) criteria (version 1.1). Adverse events were graded according to the National Cancer Institute Common Terminology Criteria for Adverse Events (NCI CTCAE), version 5.0.

Study Endpoints

The primary endpoint was the 9-month progression-free survival (PFS) rate in arm A.

Secondary endpoints included progression-free survival, overall survival (OS), objective response rate (ORR), disease control rate (DCR), duration of response (DoR), and safety.

Exploratory endpoints included radiomic analyses, circulating tumour DNA (ctDNA) profiling, T-cell receptor (TCR) repertoire analyses to investigate biological changes associated with TKI priming and potential biomarkers of clinical benefit.

Statistical analysis

The study was designed using Simon's optimal two-stage phase 2 design. The null hypothesis assumed a 9-month PFS rate of 27.1%, based on results from the FRESCO trial. The alternative hypothesis assumed a 9-month PFS rate of 55.0%, with a one-sided α of 0.05 and 90% power.

Sixteen evaluable patients were required in the first stage. If more than four patients achieved 9-month PFS, an additional nine patients would be enrolled in the second stage, yielding a total sample size of 25 patients in arm A. The primary endpoint would be considered met if more than ten patients achieved 9-month PFS. Progression-free survival was defined as the interval from the date of the first dose of

treatment to the first of either disease progression, relapse or death from any cause. Overall survival was defined as the interval from the date of the first dose of treatment to death from any cause. Patients without events were censored at the date of last follow-up.

Survival outcomes were estimated using the Kaplan–Meier method and reported with corresponding 95% confidence intervals (CIs). ORR and DCR were calculated with exact Clopper–Pearson 95% CIs. Statistical analyses were performed using SAS version 9.4.

Exploratory Biomarker Analyses

Baseline and longitudinal radiomic analyses were performed using contrast-enhanced computed tomography images. High-throughput radiomic features were extracted using PyRadiomics, and predictive models were developed to distinguish patients assigned to arm A from those assigned to arms B and C.

Peripheral blood samples collected at baseline, after one cycle of TKI treatment, and at treatment discontinuation were used for ctDNA, TCR repertoire analyses. Detailed laboratory procedures for next-generation sequencing, TCR sequencing are provided in the Supplementary Appendix.

Declarations

Acknowledgements

We are grateful to all patients and relatives who participated in this trial and all investigators and their dedicated teams for supporting this academic study.

Ethics statement

This study was conducted in accordance with the 1964 Declaration of Helsinki and its later amendments. It was approved by the Ethics Committee of Liaoning Cancer Hospital & Institute (approval no. 20200702).

Consent to participate

Written informed consent was obtained from all patients before enrollment.

Funding

This work was supported by the scientific research foundation for the introduction of talents, Liaoning Cancer Hospital & Institute (Grant Z1702); Liaoning Talent Development Plan-Medical Experts (Grants YXMJ-LJ-17 ; XLYC2512093); Liaoning Key Laboratory of Gastrointestinal Cancer Translational Research (Grant Z2202).

Conflicts of interest

The authors declare that they have no conflicts of interest.

Data availability

The de-identified participant data that support the findings of this study are not publicly available owing to institutional policy and participant confidentiality requirements, but are available from the corresponding author upon reasonable request, subject to approval by the institutional ethics committee. Requests should be directed to Prof. Jingdong Zhang (jdzhang@cancerhosp-ln-cmu.com)."

Author contributions

Qian Dong: Conceptualization, Investigation, Data curation, Patient recruitment, Writing–review & editing.

Xin Sun, Xiujie Cui, Jin Zhou, Lingshan Wang, Jian Zhang, Li Man, Yuyang Zhang, Yuanhe Wang, Tao Wu, Tiejun Chen, Yuyang Dong, Junwei Zhang, Yanyuan Huang, Siliang Wang: Investigation, Patient recruitment, Data collection.

Yanwen Diao Haobo Yin: Data curation, Investigation, Patient follow-up, Formal analysis, Statistical analysis, Visualization, Writing–original draft.

Hongming Xu, Xiaorui Ma: Methodology, Formal analysis, Radiomics analysis, Visualization.

Jingdong Zhang: Conceptualization, Methodology, Supervision, Project administration, Funding acquisition, Writing–review & editing.

All authors contributed to the study, reviewed the manuscript, and approved the final version for publication.

References

1. Yan S et al (2024) Immune checkpoint inhibitors in colorectal cancer: limitation and challenges. Front Immunol 15:1403533
2. Guven DC et al (2024) The Efficacy of Immune Checkpoint Inhibitors in Microsatellite Stable Colorectal Cancer: A Systematic Review. Oncologist 29:e580–e600
3. Le DT et al (2015) PD-1 Blockade in Tumors with Mismatch-Repair Deficiency. N Engl J Med 372:2509–2520
4. He L et al (2025) Fruquintinib Combined With PD-1 Inhibitors for the Treatment of the Patients With Microsatellite Stability Metastatic Colorectal Cancer: Real-World Data. Clin Oncol 38:103700
5. Gou M et al (2022) Fruquintinib in Combination With PD-1 Inhibitors in Patients With Refractory Non-MSI-H/pMMR Metastatic Colorectal Cancer: A Real-World Study in China. Front Oncol 12:851756
6. An T et al (2024) Fruquintinib with PD-1 inhibitors versus fruquintinib monotherapy in late-line mCRC: A retrospective cohort study based on propensity score matching. JCO 42:139–139

7. Yang X et al (2023) P-145 Efficacy, safety, and predictors of fruquintinib plus PD-1 in refractory MSS metastatic colorectal cancer in a real-world setting. Ann Oncol 34:S66
8. Wang F et al (2024) Combined anti-PD-1, HDAC inhibitor and anti-VEGF for MSS/pMMR colorectal cancer: a randomized phase 2 trial. Nat Med 30:1035–1043
9. Catalano M et al (2023) Immunotherapy-related biomarkers: Confirmations and uncertainties. Crit Rev Oncol/Hematol 192:104135
10. Yang C et al (2023) Biomarkers for immune checkpoint inhibitors in colorectal cancer: recent advances and future perspectives. Cancer Biol Med 1–7. 10.20892/j.issn.2095-3941.2023.0201
11. Fakih M et al (2023) Regorafenib plus nivolumab in patients with mismatch repair-proficient/microsatellite stable metastatic colorectal cancer: a single-arm, open-label, multicentre phase 2 study. eClinicalMedicine 58:101917
12. Fukuoka S et al (2020) Regorafenib Plus Nivolumab in Patients With Advanced Gastric or Colorectal Cancer: An Open-Label, Dose-Escalation, and Dose-Expansion Phase Ib Trial (REGONIVO, EPOC1603). JCO 38:2053–2061
13. Doleschel D et al (2021) Regorafenib enhances anti-PD1 immunotherapy efficacy in murine colorectal cancers and their combination prevents tumor regrowth. J Exp Clin Cancer Res 40:288
14. Morano F et al (2022) Temozolomide Followed by Combination With Low-Dose Ipilimumab and Nivolumab in Patients With Microsatellite-Stable, O^6 -Methylguanine–DNA Methyltransferase–Silenced Metastatic Colorectal Cancer: The MAYA Trial. JCO 40:1562–1573
15. Zhang M et al (2025) Microbiota-derived urocanic acid triggered by tyrosine kinase inhibitors potentiates cancer immunotherapy efficacy. Cell Host Microbe 33:915–931e9
16. Yang K et al (2022) Real-world outcomes of regorafenib combined with immune checkpoint inhibitors in patients with advanced or metastatic microsatellite stable colorectal cancer: A multicenter study. Cancer Immunol Immunother 71:1443–1451
17. Li J et al (2020) The Efficacy and Safety of Regorafenib in Combination With Anti-PD-1 Antibody in Refractory Microsatellite Stable Metastatic Colorectal Cancer: A Retrospective Study. Front Oncol 10:594125
18. Wang C et al (2020) Regorafenib and Nivolumab or Pembrolizumab Combination and Circulating Tumor DNA Response Assessment in Refractory Microsatellite Stable Colorectal Cancer. Oncologist 25:e1188–e1194
19. Overman MJ et al (2026) Nivolumab plus ipilimumab and cobimetinib in previously treated microsatellite-stable/DNA mismatch repair-proficient metastatic colorectal cancer: the phase II CheckMate 142 trial. ESMO Gastrointest Oncol 12:100334
20. Damato A et al (2026) First-line Nivolumab plus FOLFOXIRI/Bevacizumab in advanced RAS/BRAF-mutated colorectal cancer: efficacy, safety and biomarker discovery from the phase II NIVACOR trial. Nat Commun 17:4478
21. Ganesh K et al (2019) Immunotherapy in colorectal cancer: rationale, challenges and potential. Nat Rev Gastroenterol Hepatol 16:361–375

22. Farah H et al (2026) Overcoming conditional immune resistance in MSS and pMMR colorectal cancer: A sequential gating framework for immunotherapy. Crit Rev Oncol Hematol 223:105353
23. Yao N et al (2026) Biomarker guided combination strategies and perioperative integration for immune cold microsatellite stable colorectal cancer. Discov Oncol 17:429
24. Fukumura D, Kloepper J, Amoozgar Z, Duda DG, Jain RK (2018) Enhancing cancer immunotherapy using antiangiogenics: opportunities and challenges. Nat Rev Clin Oncol 15:325–340
25. Huang J, Chen X (2025) Tumor Cavitation with Anlotinib Treatment in Lung Adenocarcinoma. Diagnostics (Basel) 15:1280
26. Lee WS, Yang H, Chon HJ, Kim C (2020) Combination of anti-angiogenic therapy and immune checkpoint blockade normalizes vascular-immune crosstalk to potentiate cancer immunity. Exp Mol Med 52:1475–1485
27. Jain RK (2014) Antiangiogenesis strategies revisited: from starving tumors to alleviating hypoxia. Cancer Cell 26:605–622
28. Georganaki M, van Hooren L, Dimberg A (2018) Vascular Targeting to Increase the Efficiency of Immune Checkpoint Blockade in Cancer. Front Immunol 9:3081
29. Treps L (2018) EnLIGHTenment of tumor vessel normalization and immunotherapy in glioblastoma. J Pathol 246:3–6
30. Gu L et al (2026) PD-1 blockade plus tyrosine kinase inhibitor remodels the tumor microenvironment in advanced renal cell carcinoma. Nat Commun 17:4626
31. Zhu M et al (2026) Regorafenib enhances anti-PDCD1/PD-1 therapeutic efficacy in colorectal cancer by promoting SQSTM1/p62-mediated CD274/PD-L1 degradation. Autophagy 22:1203–1220

Tables

Table 1 Patient demographics and baseline disease characteristics

Characteristics	Arm A (n=25)	Arm B (n=11)	Arm C (n=22)
Median Age, years (range)	57.0 (34,74)	58.9 (38,75)	59.5 (41,72)
Sex, n (%)			
Male	15 (60.0)	6 (54.5)	13 (59.1)
Female	10 (40.0)	5 (45.5)	9 (40.9)
ECOG PS, n (%)			
0	1 (4.0)	1 (9.1)	0 (0.0)
1	24 (96.0)	10 (90.9)	22 (100.0)
Primary tumor location, n (%)			
Right colon	3 (12.0)	2 (18.2)	5 (22.7)
Left colon	22 (88.0)	9 (81.8)	17 (77.3)
Metastasis, n (%)			
Single organ metastasis	8 (32.0)	0 (0.0)	9 (40.9)
Multiple organ metastasis	17 (68.0)	11 (100.0)	13 (59.1)
Metastatic lesions, n (%)			
Liver	10 (40.0)	8 (72.7)	20 (90.9)
Lung	20 (80.0)	9 (81.8)	10 (45.5)
Lymph node	7 (28.0)	3 (27.3)	5 (22.7)
Bone	3 (12.0)	2 (18.2)	2 (9.1)
Others	5 (20.0)	2 (18.2)	3 (13.6)
RAS/BRAF status, n (%)			
RAS/BRAF^{V600E} wild-type	14 (56.0)	2 (18.2)	7 (31.8)
RAS mutant	9 (36.0)	8 (72.7)	11 (50.0)
BRAF^{V600E} mutant	2 (8.0)	0 (0.0)	0 (0.0)
Unknown	0 (0.0)	1 (9.1)	4 (18.2)
Previous systemic treatment lines, n (%)			
<3	21 (84.0)	9 (81.8)	14 (63.6)
≥3	4 (16.0)	2 (18.2)	8 (36.4)
Prior chemecotherapeutic agents, n (%)			

Fluoropyrimidine	25 (100.0)	11 (100.0)	22 (100.0)
Oxaliplatin	25 (100.0)	11 (100.0)	22 (100.0)
Irinotecan	25 (100.0)	11 (100.0)	22 (100.0)
Prior targeted therapeutic agents, n (%)			
Bevacizumab	16 (64.0)	10 (90.9)	15 (68.2)
Cetuximab	11 (44.0)	2 (18.2)	7 (31.8)
Primary tumor resected , n (%)			
Yes	23 (92.0)	8 (72.7)	9 (40.9)
No	2 (8.0)	3 (27.3)	13 (59.1)
Type of differentiated, n (%)			
Moderately differentiated	17 (68.0)	10 (90.9)	11 (50.0)
Poorly differentiated	7 (28.0)	1 (9.1)	6 (27.3)
Unknown	1 (4.0)	0 (0.0)	5 (22.7)
Tumour stage at screening, n(%)			
II A	1 (4.0)	1 (9.1)	0 (0.0)
II B	2 (8.0)	1 (9.1)	1 (4.5)
III A	1 (4.0)	0 (0.0)	0 (0.0)
III B	2 (8.0)	2 (18.2)	0 (0.0)
III C	6 (24.0)	2 (18.2)	3 (13.6)
IV	13 (52.0)	5 (45.5)	18 (81.8)

Abbreviations: ECOG PS, Eastern Cooperative Oncology Group performance status; IQR, interquartile range;

Table 2. Treatment-Related Adverse Events During the First Treatment Part or in the Second Treatment Part

AE, no. of patients (%)	Any grade	Grade ≥ 3
Palmar–plantar erythrodysesthesia syndrome	8 (32.0)	3 (12.0)
Hypertension	7 (28.0)	4 (16.0)
Proteinuria	6 (24.0)	1 (4.0)
Hypothyroidism	6 (24.0)	1 (4.0)
Hoarseness	4 (16.0)	0 (0.0)
Fatigue	3 (12.0)	1 (4.0)
Pneumonitis	3 (12.0)	0 (0.0)
Oral mucositis /Stomatitis	2 (8.0)	2 (8.0)
Hyperthyroidism	2 (8.0)	0 (0.0)
Myocarditis	2 (8.0)	1 (4.0)
Myositis	2 (8.0)	1 (4.0)
Hepatic dysfunction / Elevated liver enzymes	2 (8.0)	0 (0.0)
Elevated serum creatinine	1 (4.0)	1 (4.0)
Lower gastrointestinal bleeding	1 (4.0)	0 (0.0)
Weight loss	1 (4.0)	0 (0.0)
Arthralgia	1 (4.0)	0 (0.0)
Anorexia / Decreased appetite	1 (4.0)	0 (0.0)
Hypophysitis	1 (4.0)	0 (0.0)
Rash	1 (4.0)	0 (0.0)
Intestinal obstruction	1 (4.0)	1 (4.0)
Adrenal insufficiency	1 (4.0)	0 (0.0)

Abbreviation: AE, adverse event.

Figures

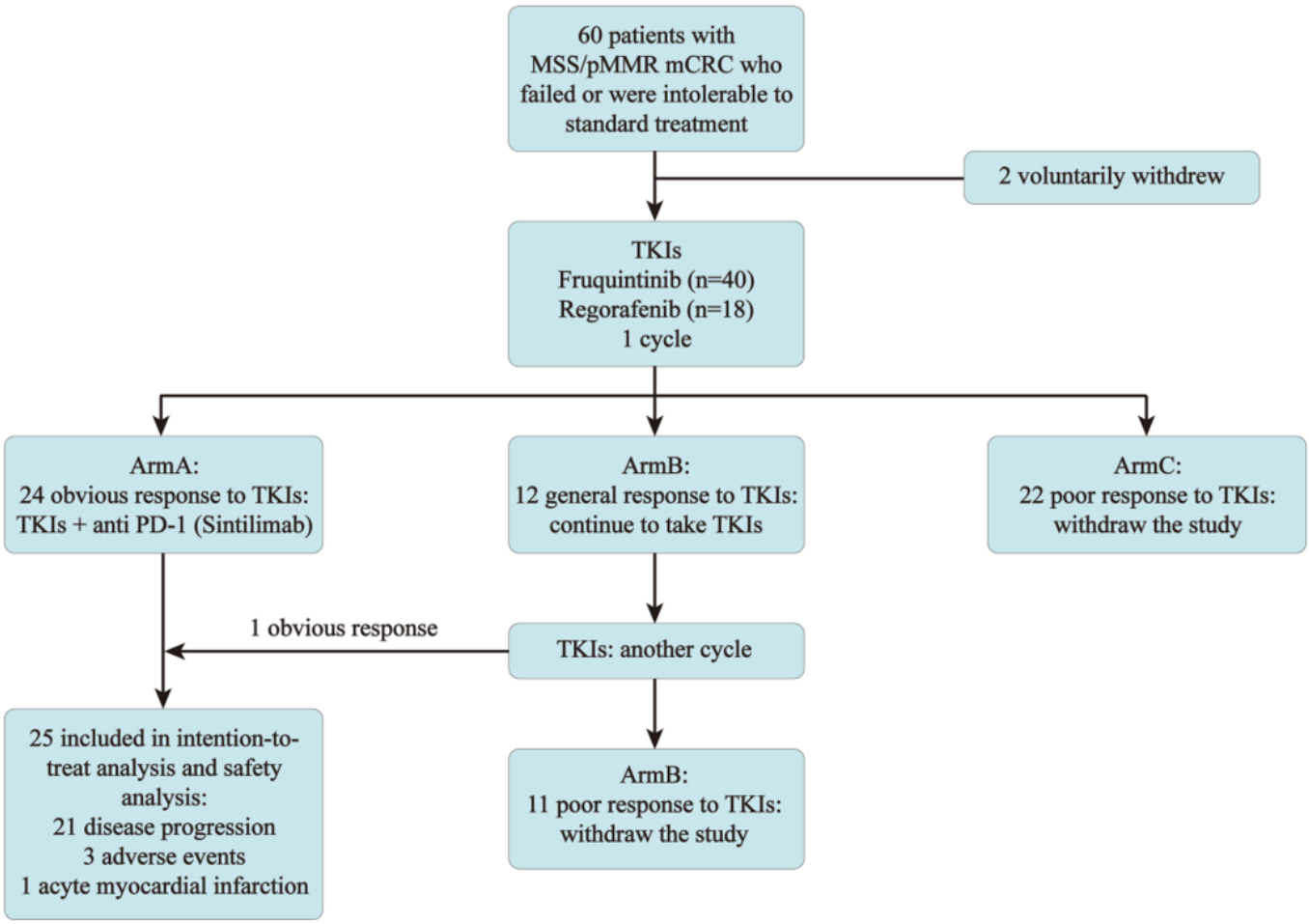


Figure 1

Flow diagram of the trial process. A total of 60 patients were recruited from eight Chinese medical institutions between 10 March 2021 and 24 June 2024 and received the study treatment. The participants were divided into three arms according to their response to TKIs. Response classifications were based on the revised Response Evaluation Criteria in Solid Tumours (RECIST), v. 1.1. Arm A: Obvious response to TKIs, including reduction in the diameter of the target lesion(s), complete response (CR), partial response (PR) or shrunken stable disease (SD) Patients without progressive disease (non-PD) exhibiting radiographic changes suggestive of treatment response according to Choi criteria, such as cavitation of solid metastatic lung lesions or a ≥15% decrease in metastatic liver lesion density were also placed in arm A. Arm B: General response to TKIs, including enlarged SD, but without the radiographic features of patients in arm A. Arm C: Poor response to TKIs, including disease progression.

mCRC, metastatic colorectal adenocarcinoma; MSS/pMMR, microsatellite stable/ proficient mismatch repair; PD-1, programmed cell death protein 1; TKIs, tyrosine kinase inhibitors

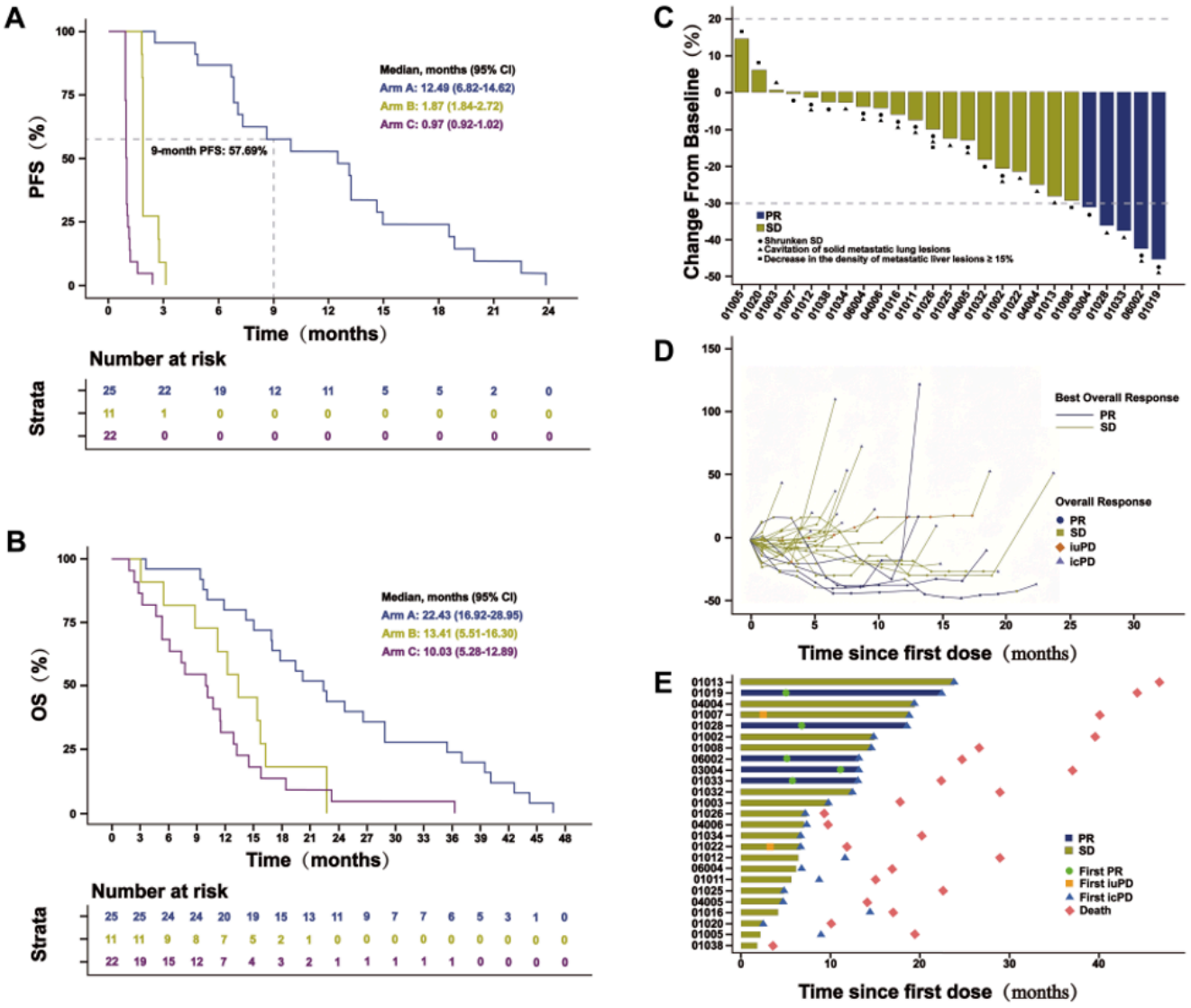


Figure 2

Kaplan—Meier curves for (**a**) PFS and (**b**) OS of patients in the treatment group. (**c**) Waterfall plot of the best tumour responses achieved by each patient; (**d**) Spider plot of participants' tumour response dynamics; (**e**) Swimmer plot of each patient's treatment duration, with the occurrence times of the first PR, first iuPD, first icPD and death.

OS, overall survival; PFS, progression-free survival; icPD, immune-confirmed progressive disease; iuPD, immune-unconfirmed progressive disease; PFS, progression-free survival; PR, partial response; SD, stable disease

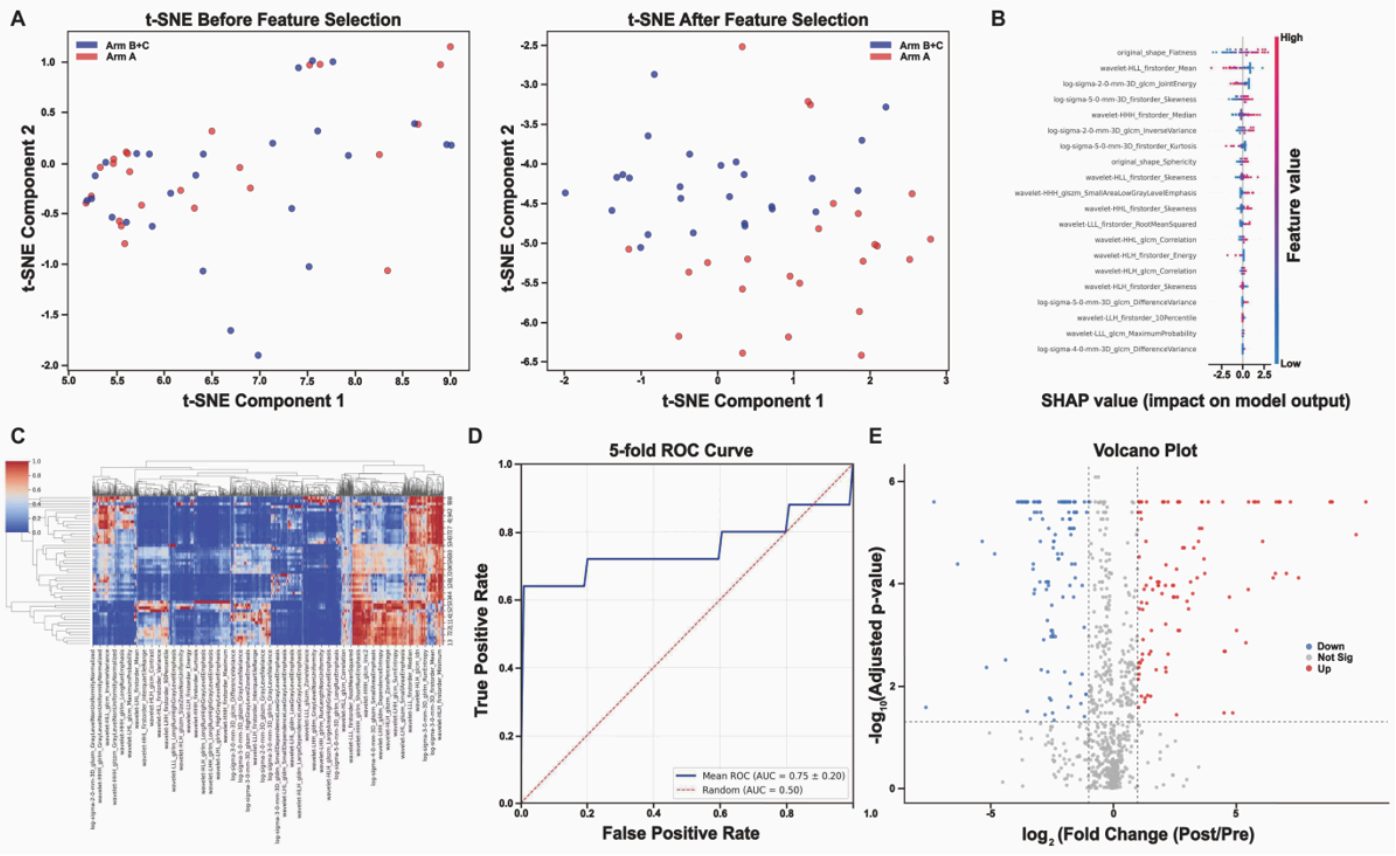


Figure 3

Development and validation of the baseline radiomics model and dynamic radiomic alterations following TKI treatment.(A) t-distributed stochastic neighbor embedding (t-SNE) visualization of patients in Arm A and Arm B+C before and after radiomic feature selection. Feature selection improved the separation between patients who subsequently benefited from sequential TKI–immunotherapy treatment (Arm A) and those who did not (Arm B+C). (B) SHAP summary plot showing the contribution of the selected radiomic features to model prediction. Features are ranked according to their impact on model output, with color indicating feature value and SHAP value indicating the direction and magnitude of contribution. (C) Hierarchical clustering heatmap of the selected radiomic features. Columns represent radiomic features and rows represent individual patients. Color intensity indicates normalized feature values. (D) Receiver operating characteristic (ROC) curves from five-fold cross-validation of the radiomics model. The model achieved a mean area under the curve (AUC) of 0.75 ± 0.20 for distinguishing Arm A from Arm B+C. (E) Volcano plot showing differential radiomic features between pre- and post-TKI treatment images in Arm A. Red and blue dots indicate significantly upregulated and downregulated features, respectively, after multiple-testing correction. Significant changes were predominantly observed in density-related, heterogeneity-related, and wavelet-/LoG-derived multi-scale texture features.

AUC, area under the curve; ROC, receiver operating characteristic; SHAP, Shapley Additive Explanations; t-SNE, t-distributed stochastic neighbor embedding; TKI, tyrosine kinase inhibitor.

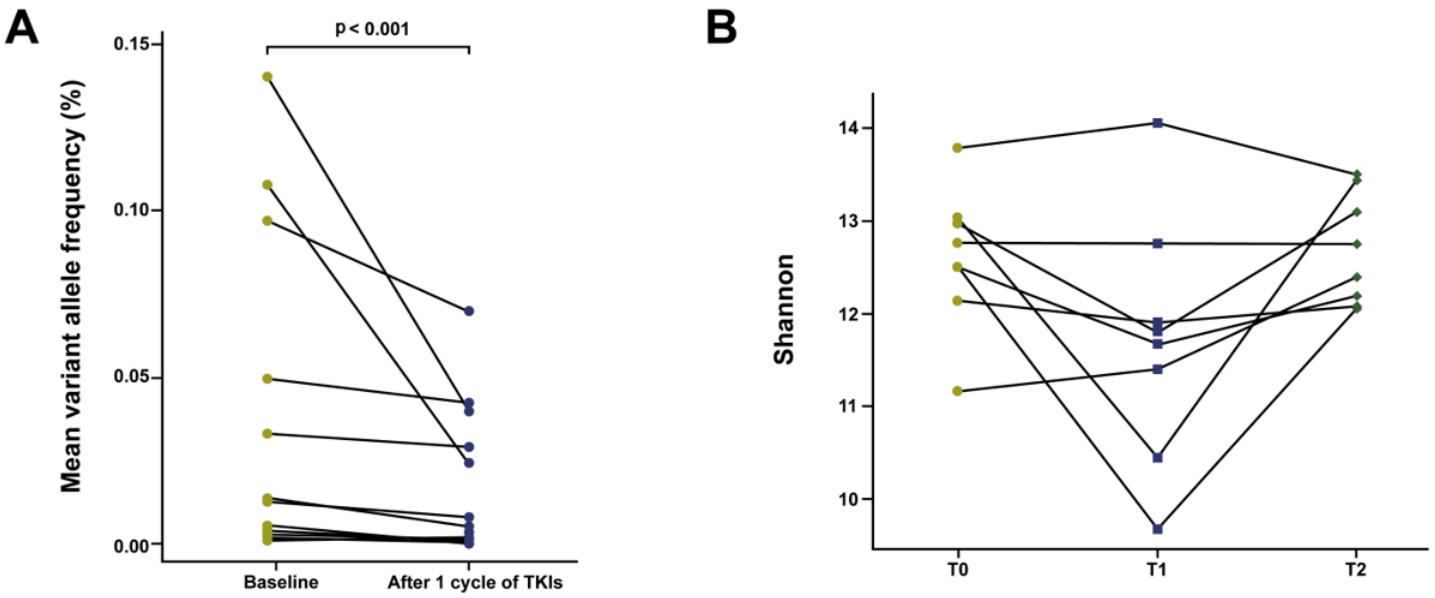


Figure 4

(A) Longitudinal changes in plasma circulating tumor DNA (ctDNA) allele frequency (AF) at baseline (T0), after one cycle of TKI treatment (T1), and at study end (T2). Each line represents an individual patient, showing temporal dynamics of tumor-derived mutational burden under sequential TKI-based therapy. (B) Temporal evolution of T-cell receptor (TCR) repertoire diversity, quantified by the Shannon diversity index, at the corresponding time points (T0, T1, and T2). Each line represents an individual patient, showing longitudinal changes in TCR clonal diversity during sequential TKI-based therapy.

Supplementary Files

This is a list of supplementary files associated with this preprint. Click to download.

- SupplementaryAppendix.pdf
- CONSORT2025checklistfilledTRAP.pdf
- FigureS1S2S3.docx